NASA/TP-1998-206559

Anomalous Buckling Characteristics of Laminated Metal-Matrix Composite Plates With Central Square Holes

William L. Ko
Dryden Flight Research Center
Edwards, California

National Aeronautics and
Space Administration

Dryden Flight Research Center
Edwards, California 93523-0273

July 1998

NOTICE

Use of trade names or names of manufacturers in this document does not constitute an official endorsement of such products or manufacturers, either expressed or implied, by the National Aeronautics and Space Administration.

Available from the following:

NASA Center for AeroSpace Information (CASI)
7121 Standard Drive
Hanover, MD 21076-1320
(301) 621-0390

National Technical Information Service (NTIS)
5285 Port Royal Road
Springfield, VA 22161-2171
(703) 487-4650

ABSTRACT

Compressive buckling analysis was performed on metal-matrix composite (MMC) plates with central square holes. The MMC plates have varying aspect ratios and hole sizes and are supported under different boundary conditions. The finite-element structural analysis method was used to study the effects of plate boundary conditions, plate aspect ratio, hole size, and the composite stacking sequence on the compressive buckling strengths of the perforated MMC plates. Studies show that by increasing the hole sizes, compressive buckling strengths of the perforated MMC plates could be considerably increased under certain boundary conditions and aspect ratios ("anomalous" buckling behavior); and that the plate buckling mode could be symmetrical or antisymmetrical, depending on the plate boundary conditions, aspect ratio, and the hole size. For same-sized plates with same-sized holes, the compressive buckling strengths of the perforated MMC plates with $[90/0/0/90]_2$ lamination could be as much as 10 percent higher or lower than those of the $[45/-45/-45/45]_2$ laminations, depending on the plate boundary conditions, plate aspect ratios, and the hole size. Clamping the plate edges induces far stronger "anomalous" buckling behavior (enhancing compressive buckling strengths at increasing hole sizes) of the perforated MMC plates than simply supporting the plate edges.

NOMENCLATURE

ANTI	antisymmetric
c	length of square hole side, in.
E_L	lamina Young's modulus in fiber direction, lb/in^2
E_T	lamina Young's modulus in direction transverse to fiber direction, lb/in^2
E43	quadrilateral combined membrane and bending element
G_{LT}	lamina shear modulus, lb/in^2
JLOC	joint location (or grid point, or node)
l	length of laminated composite plate, in.
MMC	metal-matrix composite
N_y	compressive force intensity in y direction, lb/in
$(N_y)_{cr}$	critical value of N_y at buckling, lb/in
SPAR	Structural Performance and Resizing (finite-element computer program)
SYM	symmetric
t	thickness of laminated composite plate, in.
t'	lamina thickness, in.
w	width of laminated composite plate, in.
x, y	rectangular Cartesian coordinates
ν_{LT}	lamina Poisson ratio

INTRODUCTION

In aerospace structures, cutouts are commonly found as access ports for mechanical and electrical systems, or simply to reduce weight. Those structural panels with cutouts are often subjected to compressive loads and could buckle if overloaded. Therefore, the buckling characteristics of those structural panels with cutouts must be fully understood to obtain knowledge for efficient structural design.

For a uniformly compressed solid rectangular plate, the closed-form buckling solutions are easily obtained because the prebuckling stress field is uniform everywhere in the plates.[1] When a hole is introduced into the plate, the buckling strength is influenced by the loss in bending stiffness (in the cutout region) and by the redistribution of the prebuckling stress field. This stress field is nonuniform because of the creation of traction-free hole boundary. The buckling analysis then becomes more cumbersome, and the explicit closed-form buckling solutions are almost unattainable. In the past, therefore, various approximate methods had to be formulated to numerically obtain the buckling solutions for the perforated plates under uniform compression.

Buckling behavior of flat plates (isotropic and anisotropic) with central cutouts (circular, elliptic, and square holes) has been studied theoretically and experimentally by many authors.[2–19] Most of these studies focused on the compressive buckling of simply supported square plates with central holes, and observed that introducing the cutouts always decreased the buckling strengths of the perforated plates. This observation seemed to agree with the intuition that introducing a large hole into a compressively loaded plate could cause a reduction in the buckling strength of the perforated plates because of the loss of bending strength resulting from the loss of cutout material. Such buckling behavior, however, may not always be the case for other plate geometry (i.e., aspect ratio, hole size) and boundary conditions. In theoretical and experimental studies of buckling behavior of isotropic plates with holes, Ritchie and Rhodes[8] have shown that introducing a hole into a plate did not always reduce the buckling load and, in some instances, could increase its buckling strength—the "anomalous" buckling behavior of the perforated plates. Nemeth[12, 13] also observed a similar phenomenon and has found that, contrary to the conventional intuition, under certain sets of geometrical and boundary conditions, the buckling strengths of the square and rectangular plates with central circular and square holes did increase as the hole size increased. Such "anomalous" buckling characteristics of the perforated plates are a very useful structural property in the practical applications and deserve extensive study to fully understand this phenomenon.

Using a well-developed finite-element structural analysis computer program to calculate the prebuckling stresses and obtain the buckling eigenvalue solutions, the effect of the plate geometry (i.e., aspect ratio, hole size, hole shape) and the plate boundary conditions on the mechanical and thermal buckling strengths of square and rectangular isotropic plates containing central circular and square holes was extensively studied.[20] The study revealed that clamping the plate boundaries strongly affects increases in the buckling strength for large hole sizes, and that for the same-sized plates and same cutout areas, the square hole cases exhibited slightly stronger "anomalous" buckling behavior. This buckling study needed to be extended to the cases of laminated composite plates with cutouts.

This report describes the compressive buckling analysis of laminated metal-matrix composite (MMC) plates with square holes. A finite-element method was used to study the effects of plate aspect ratio, hole size, plate boundary conditions, and composite stacking sequence on the compressive buckling strengths of the perforated MMC plates. This report presents the results of such buckling analysis, and discusses in detail the "anomalous" buckling behavior of the perforated MMC plates.

DESCRIPTION OF PROBLEM

Geometry of the MMC plates with central cutouts is described below. The four cases of boundary conditions used in the finite-element analysis are also described.

Geometry

Figure 1 shows the geometry of MMC plates (length, l; width, w; and thickness, t) containing a central square hole with side length c. The perforated MMC plates have $[90/0/0/90]_2$ and $[45/-45/-45/45]_2$ laminations with the fiber orientation angles measured from the x axis.

The square-hole geometry is chosen instead of circular-hole because it is easier to generate a family of finite-element models of different aspect ratios and different hole sizes without distorting the finite-element mesh (for the circular holes, each time the hole size is changed, a new finite-element mesh must be generated to maintain proper element aspect ratios). The square-hole geometry is also chosen because, for the same-sized plates with the same cutout areas, the square-hole cases exhibited slightly stronger "anomalous" buckling behavior than the circular-hole cases.[20]

Table 1 shows the dimensions of a family of perforated MMC plates analyzed. Notice that all the plates have the same width (w = 20 in.) and the same thickness (t = 0.064 in.).

Table 1. Dimensions of perforated MMC plates analyzed.

w, in.	t, in.	l/w	c/w
20	0.064	1.0	0 ~ 0.7
20	0.064	1.5	0 ~ 0.7
20	0.064	2.0	0 ~ 0.7

where the range "c/w = 0 ~ 0.7" implies c/w = 0.00, 0.05, 0.10, 0.15, 0.20, 0.25, 0.30, 0.35, 0.40, 0.45, 0.50, 0.55, 0.60, 0.65, 0.70.

For a given plate aspect ratio, the 15 hole-size cases (table 1) will provide 15 data points for plotting each buckling curve in the plots showing $(N_y)_{cr}$ as a function of c/w. However, if the buckling curve has any sharp bends in certain regions, additional data points (for c/w values not listed in table 1) are generated to define those sharp-bend regions more precisely.

Boundary Conditions

The perforated MMC plates are subjected to uniform compression in the y direction (fig. 2). The four edges of the perforated plates are either simply supported or clamped. The two axes of symmetry (i.e., x and y axes) of the plate have no in-plane motions. The lower and the upper horizontal edges of the plate are free to move in the loading direction (y direction). The two unloaded edges are either constrained from the transverse in-plane motion (defined as fixed case) (fig. 2(a)), or unconstrained from the transverse

inplane motion (defined as free case) (fig. 2(b)). The four cases of boundary conditions considered in the buckling analysis are as follows:

- 4S-fixed: four edges simply supported; the two side edges can slide freely along the lubricated fixed guides (fig. 3(a)).
- 4S-free: four edges simply supported; the two side edges can slide freely along the lubricated guides, which can have free in-plane transverse motions (fig. 3(b)).
- 4C-fixed: four edges clamped; the two side edges can slide freely along the lubricated fixed clamping guides (fig. 3(c)).
- 4C-free: four edges clamped; the two side edges can slide freely along the lubricated clamping guides, which can have free in-plane transverse motions (fig. 3(d)).

Figure 4 shows the degrees of freedom constrained on the axes of symmetry and at the boundaries of the plates for the above four cases of boundary conditions.

FINITE-ELEMENT ANALYSIS

This section describes the finite-element modeling of the perforated MMC plates. The composite material and geometrical properties used in the finite-element linear elastic buckling analysis are also given.

Finite-Element Modeling

In the finite-element linear elastic buckling analysis, the Structural Performance and Resizing (SPAR) finite-element computer program[21] was used to calculate symmetrical and antisymmetrical buckling loads and to plot the buckling mode shapes. Because of symmetry with respect to the x and y axes (fig. 1), only the first quadrant of the perforated plates was modeled with quadrilateral combined membrane and bending elements (E43 elements). The lamination section properties for E43 elements were generated by combining lamina material and geometrical properties (i.e., lamina fiber orientation angle, lamina thickness, and lamina offset distance from the middle plane of the laminated plate). Figure 5 shows a typical quarter-panel finite-element model generated for a MMC plate of aspect ratio l/w = 1.5 with square-hole size c/w = 0.2.

For each plate aspect ratio, a basic finite-element model for the unperforated plate (c/w = 0) was generated first. The finite-element models with different hole sizes were then generated from this basic model by simply removing the proper number of E43 elements from the plate central region to create the desired hole cavities. Also, to increase aspect ratios of the models, additional E43 elements were attached to the square plate models. Table 2 shows the sizes of the basic finite-element models from which a family of perturbed models was generated.

Table 2. Sizes of the basic finite-element models (c/w = 0).

l/w	JLOC	E43
1.0	441	400
1.5	651	600
2.0	861	800

Material Properties

Table 3 shows the lamina material and geometrical properties of a typical titanium matrix MMC used as input data for the E43 elements with $[90/0/0/90]_2$ and $[45/-45/-45/45]_2$ laminations.

Table 3. Material and geometrial properties of MMC lamina.

E_L, lb/in^2	E_T, lb/in^2	G_{LT}, lb/in^2	ν_{LT}	t', in.
27.7200×10^6	18.0900×10^6	8.1500×10^6	0.3000	0.0080

RESULTS

The results of the finite-element buckling analysis of the laminated MMC plates with central square holes are presented in the following subsections. Solution accuracy, fixed cases, and free cases are discussed.

Solution Accuracy

To check the accuracy of the finite-element buckling solutions, square plates with $[90/0/0/90]_2$ lamination subject to a 4S-free boundary condition were considered. The element density of the original square model (400 elements; $c/w = 0$) (table 2) was increased to 900 elements ($c/w = 0$) to find out how much the solutions will change if the element density is increased. Table 4 shows the resulting finite-element buckling solutions for the two element density cases. The numerical differences of the two sets of buckling solutions are highlighted with double underlines.

Table 4. Comparison of buckling loads $(N_y)_{cr}$ calculated using finite-element models with different element densities; $[90/0/0/90]_2$ lamination.

	$(N_y)_{cr}$, lb/in							
Element density, ($c/w = 0$)	$c/w = 0.0$	0.1	0.2	0.3	0.4	0.5	0.6	0.7
400	49.2285	46.9577	42.8246	39.6540	37.6857	36.4454	35.5917	35.1734
900	49.2286	46.9455	42.8393	39.6854	37.7255	36.4901	35.6396	35.2243
difference, percent	0.0002	0.0260	0.0343	0.0791	0.1055	0.1255	0.1344	0.1445

Table 4 shows that the buckling solutions improved negligibly although the element density was increased by 2.25 times. The solution difference increases with increased hole size; however, the difference is still infinitesimal. This close correlation of the two sets of solutions provides confidence that

the finite-element buckling solutions calculated using the original element densities (table 2) are quite accurate.

Fixed Cases

Figures 6 to 11 respectively show the symmetrical and antisymmetrical buckling loads $(N_y)_{cr}$ plotted as functions of hole size c/w (figs. 6, 8, and 10), and the associated buckling mode shapes (figs. 7, 9, and 11) for the perforated MMC plates of different laminations subject to 4S-fixed and 4C-fixed boundary conditions. The buckling strengths of $[90/0/0/90]_2$ and $[45/-45/-45/45]_2$ laminations are relatively close. The overall buckling behavior of the perforated MMC plates is very similar to that of the corresponding monolithic isotropic plates previously reported.[20]

The 4S-Fixed Cases

For the 4S-fixed cases, the antisymmetrical buckling curves always lie above the symmetrical buckling curves for all the plate aspect ratios and hole sizes (figs. 6, 8, and 10). The lowest buckling mode shapes, therefore, are always symmetrical (figs. 7(a), 9(a), and 11(a)). The buckling strengths of $[90/0/0/90]_2$ and $[45/-45/-45/45]_2$ laminations are very close for aspect ratios $l/w = 1$ (fig. 6) and $l/w = 1.5$ (fig. 8). At aspect ratio $l/w = 2$ (fig. 10), the $[90/0/0/90]_2$ lamination exhibits slightly higher buckling strengths (a maximum of 6 percent higher) (fig. 10) than the $[45/-45/-45/45]_2$ lamination.

For the 4S-fixed cases, the lowest buckling loads $(N_y)_{cr}$ (symmetrical buckling) for the square plates (fig. 6) monotonically decrease slightly from the solid plate values as the hole sizes increase, and never exhibit "anomalous" buckling behavior. For the rectangular plates (figs. 9 and 11), the symmetrical buckling loads $(N_y)_{cr}$ decrease slightly as the hole size grows, reaching minimum values at the hole sizes $c/w \approx 0.35$ to 0.40. Then, at hole sizes greater than $c/w \approx 0.40$, the buckling loads $(N_y)_{cr}$ increase slowly as the hole sizes become larger.

The 4C-Fixed Cases

For the 4C-fixed cases, strong "anomalous" buckling behavior resulted for all plate aspect ratios (figs. 6, 8, and 10). The symmetrical and antisymmetrical buckling curves entangle each other (or mutually intersect), causing the buckling curves for the lowest $(N_y)_{cr}$ values to be composite curves consisting of symmetrical and antisymmetrical buckling curves segments. Thus, the buckling mode shapes can be either symmetrical or antisymmetrical (figs. 7(b), 9(b), and 11(b)), depending on the hole sizes and the plate aspect ratios. For the 4C-fixed cases, the $[90/0/0/90]_2$ laminations have slightly higher buckling strengths (a maximum of 5 percent higher) (fig. 8) than the $[45/-45/-45/45]_2$ laminations for all the plate aspect ratios and most hole sizes. For larger holes, the secondary (or local) buckling modes start to appear at the hole boundaries (figs. 7(b), 9(b), and 11(b)); therefore, the plate buckling mode shapes exhibit the combinations of both global and local buckling modes.

For the square plate (fig. 6) of the 4C-fixed case, the lowest buckling loads $(N_y)_{cr}$ for both types of laminations decrease from their respective solid plate ($c/w = 0$) values as the hole starts to initiate and grows in size, reach their respective minimum values near the hole sizes $c/w = 0.175$, and then continue to increase and alternatively change buckling mode at hole sizes larger than 0.175. At hole sizes greater than

$c/w = 0.3$, the buckling loads $(N_y)_{cr}$ for both laminations exceed the values of corresponding solid square plates ($c/w = 0$).

For the rectangular plates (figs. 8 and 10) of the 4C-fixed cases, the lowest buckling loads $(N_y)_{cr}$ increase initially as the holes start to grow in size, then change mode and reach their respective minimum values at approximately $c/w = 0.15$. At hole sizes greater than $c/w = 0.30$, the $(N_y)_{cr}$ values exceed their respective values of the solid rectangular plates ($c/w = 0$). Rectangular plates with aspect ratio $l/w = 1.5$ (fig. 8) exhibit the strongest "anomalous" buckling behavior.

Free Cases

Figures 12 to 17 respectively show the changes of the compressive buckling loads $(N_y)_{cr}$ with the hole size c/w (figs. 12, 14, and 16), and the associated buckling mode shapes (figs. 13, 15, and 17) of the laminated MMC plates subject to 4S-free and 4C-free boundary conditions. Again, the buckling strengths of $[90/0/0/90]_2$ and $[45/-45/-45/45]_2$ laminations are quite close. The overall buckling behavior of the laminated MMC plates with square holes resemble the corresponding monolithic isotropic cases reported previously.[20]

The 4S-Free Cases

For the 4S-free cases (figs. 12, 14, and 16), the $[45/-45/-45/45]_2$ lamination exhibits slightly higher buckling strengths (symmetrical) (a maximum 10 percent higher) (fig. 12) than the $[90/0/0/90]_2$ lamination for all plate aspect ratios. For the 4S-free square plate cases (fig. 12), the symmetrical and antisymmetrical buckling curves square never intersect, and the buckling modes are always symmetrical. The buckling loads $(N_y)_{cr}$ decrease monotonically as the hole sizes increase (no "anomalous" buckling behavior). For the rectangular plates (figs. 14 and 16) under 4S-free conditions, relatively weak "anomalous" buckling behavior appeared, and the symmetrical and antisymmetrical buckling curves intersect each other at certain hole sizes, causing the buckling mode shapes to change alternately between symmetrical and antisymmetrical modes as the hole sizes change.

The 4C-Free Cases

For the 4C-free cases (figs. 12, 14, and 16), the symmetrical and antisymmetrical buckling curves for all plate aspect ratios entangle each other, causing the actual buckling curves to be symmetrical/antisymmetrical composite curves. The buckling strengths of $[90/0/0/90]_2$ lamination are slightly higher or lower (a maximum of 3 percent difference) (figs. 12 and 14) than the $[45/-45/-45/45]_2$ lamination, depending on the hole sizes.

For the square plate (fig. 12), the lowest buckling loads $(N_y)_{cr}$ for the 4C-free cases decrease (with slight waves) as hole size decreases, never increase with the hole size, and do not show "anomalous" buckling behavior. For the rectangular plates (figs. 14 and 16), the buckling loads $(N_y)_{cr}$ for 4C-free cases increase at large hole sizes, showing strong "anomalous" buckling behavior. For the 4C-free cases, the buckling mode shapes of the MMC plates with large holes (figs. 13, 15, and 17) show complex buckling modes consisting of global and pronounced local buckling at the hole boundaries.

DISCUSSION

The buckling behavior of MMC plates with central square holes, like the corresponding monolithic isotropic cases,[20] exhibit "anomalous" buckling behavior under certain boundary conditions (especially cases with clamped edges), hole sizes, and plate aspect ratios. That is, the compressive buckling strengths of the perforated MMC plates can increase rather than decrease as the hole sizes grow larger. As the hole sizes increase, the plates lose more material and consequently lose more bending stiffness. The buckling strengths are therefore expected to decrease as the hole sizes increase. This conventional notion turned out not to be always true, as shown in this report. Such "anomalous" buckling behavior of the perforated plates could be explained as follows.

When the hole size becomes considerably larger in relation to the plate width, most of the compressive load is carried by the two narrow side strips of material along the plate load-free boundaries. A stronger plate boundary condition (i.e., clamped rather than simply supported boundaries) increases the buckling strength, but the higher stress concentration could reduce the buckling strength. Thus, whichever effect is dominant will determine the increase or decrease of the buckling loads of the perforated MMC plates at increasing hole sizes.

This "anomalous" buckling characteristics of the perforated MMC plates has very useful applications in the aerospace compression panel design. By cutting central holes of proper sizes in the compression panels for weight reduction, the compressive buckling strengths of the panels can simultaneously be enhanced.

CONCLUDING REMARKS

Finite-element compressive buckling analysis was performed on metal-matrix composite (MMC) plates containing central square holes. The effects of plate aspect ratio, hole size, plate boundary conditions, and the composite stacking sequence on the compressive buckling strengths and buckling mode shapes were studied in detail. The key findings of the analysis are as follows:

- Increasing hole size does not necessarily reduce the compressive buckling strengths of the perforated MMC plates. For certain plate aspect ratios and plate boundary conditions, the compressive buckling strengths could increase at large hole sizes ("anomalous" buckling behavior).
- The buckling mode shapes of the perforated MMC plates can be symmetrical or antisymmetrical depending on the plate aspect ratio, hole size, and plate boundary condition.
- The buckling strengths of perforated MMC plates with $[90/0/0/90]_2$ lamination could be higher or lower, by as much as 10 percent, than those with $[45/-45/-45/45]_2$ lamination, depending on the plate aspect ratio, plate boundary conditions, and hole size.
- Clamping the edges strongly enhances the "anomalous" buckling behavior (i.e., enhancing compressive buckling strengths at increasing hole sizes) of the perforated MMC plates compared with simply supporting the edges.

Dryden Flight Research Center
National Aeronautics and Space Administration
Edwards, California, December 16, 1997

REFERENCES

1. Timoshenko, Stephen P. and James M. Gere, *Theory of Elastic Stability*, 2nd edition, McGraw-Hill Book Company, New York, 1961.

2. Levy, Samuel, Ruth M. Woodley, and Wilhelmina D. Kroll, "Instability of Simply Supported Square Plate With Reinforced Circular Hole in Edge Compression," *Journal of Research*, National Bureau of Standards, vol. 39, research paper no. RP1849, Dec. 1947, pp. 571–577.

3. Kumai, Toyoji, "Elastic Stability of the Square Plate with a Central Circular Hole Under Edge Thrust," *Proc. Japan Nat. Cong. Appl. Mech.*, 1951, pp. 81–88.

4. Schlack, Alois L., Jr., "Elastic Stability of Pierced Square Plates," *Experimental Mechanics*, June 1964, pp. 167–172.

5. Schlack, Alois L., Jr., "Experimental Critical Loads for Perforated Square Plates," *Experimental Mechanics*, Feb. 1968, pp. 69–74.

6. Kawai, T. and H. Ohtsubo, "A Method of Solution for the Complicated Buckling Problems of Elastic Plates With Combined Use of Rayleigh-Ritz's Procedure in the Finite Element Method," AFFDL-TR-68-150, 1968.

7. Yu, Wei-Wen and Charles S. Davis, "Cold-Formed Steel Members With Perforated Elements," *J. Structural Division*, ASCE, vol. 99, no. ST10, Oct. 1973, pp. 2061–2077.

8. Ritchie, D. and J. Rhodes, "Buckling and Post-Buckling Behavior of Plates With Holes," *Aeronautical Quarterly*, vol. 26, Nov. 1975, pp. 281–296.

9. Nemeth, Michael Paul, "Buckling Behavior of Orthotropic Composite Plates With Centrally Located Cutouts," Ph. D. Dissertation, Virginia Polytechnic Institute and State University, May 1983.

10. Nemeth, Michael P., *A Buckling Analysis for Rectangular Orthotropic Plates With Centrally Located Cutouts*, NASA-TM-86263, 1984.

11. Nemeth, Michael P., Manuel Stein, and Eric R. Johnson, *An Approximate Buckling Analysis for Rectangular Orthotropic Plates With Centrally Located Cutouts*, NASA-TP-2528, Feb. 1986.

12. Nemeth, M. P., "Buckling Behavior of Compression-Loaded Symmetrically Laminated Angle-Ply Plates With Holes," *AIAA Journal*, vol. 26, no. 3, Mar. 1988, pp. 330–336.

13. Nemeth, Michael P., "Buckling and Postbuckling Behavior of Compression-Loaded Isotropic Plates With Cutouts," *31st AIAA/ASME/ASCE/AHS/ASC Structures, Structural Dynamics and Materials Conference*, AIAA-90-0965-CP, Apr. 1990, pp. 862–876.

14. Lee, Y. J., H. J. Lin, and C. C. Lin, "A Study on the Buckling Behavior of an Orthotropic Square Plate With a Central Circular Hole," *Composite Structures*, vol. 13, no. 3, 1989, pp.173–188.

15. Britt, V. O., "Shear and Compression Buckling Analysis for Anisotropic Panels With Centrally Located Elliptical Cutouts," *34th AIAA/ASME/ASCE/AHS/ASC Structures, Structural Dynamics and Materials Conference*, AIAA-93-1565-CP, Apr. 1993, pp. 2240–2249.

16. Vandenbrink, Dennis J. and Manahar P. Kamat, "Post-Buckling Response of Isotropic and Laminated Composite Square Plates With Circular Holes," *Finite Elements in Analysis and Design*, vol. 3, Oct. 1987, pp. 165–174.

17. Yasui, Yoshiaki and Kiyoshi Tsukamura, "Buckling Strength of Rectangular FRP Plate With a Hole (In the Case of CFRP and GFRP Cross-Ply Laminated Plate)," *J. Japan Society of Materials Science*, vol. 37, Sept. 1988, pp. 1050–1056.

18. Weijia, Cao, "Finite Element Analysis and Experimental Verification of the Elasto-Plastic Buckling of the Wing-Webs With Holes," *Proceedings of the International Conference on Nonlinear Mechanics*, Oct. 1985, pp. 444–448.

19. Ter-Emmanuil'ian, N. la., "Stability of an Orthotropic Flexible Square Plate With a Square Hole," *Mekhanika Polimerov*, vol. 7, May–June 1971, pp. 482–488.

20. Ko, William L., *Mechanical- and Thermal-Buckling Behavior of Rectangular Plates With Different Central Cutouts*, NASA-TM-1998-206542, 1998.

21. Whetstone, W. D., *SPAR Structural Analysis System Reference Manual: System Level 13A, vol. 1, Program Execution*, NASA-CR-158970-1, Dec. 1978.

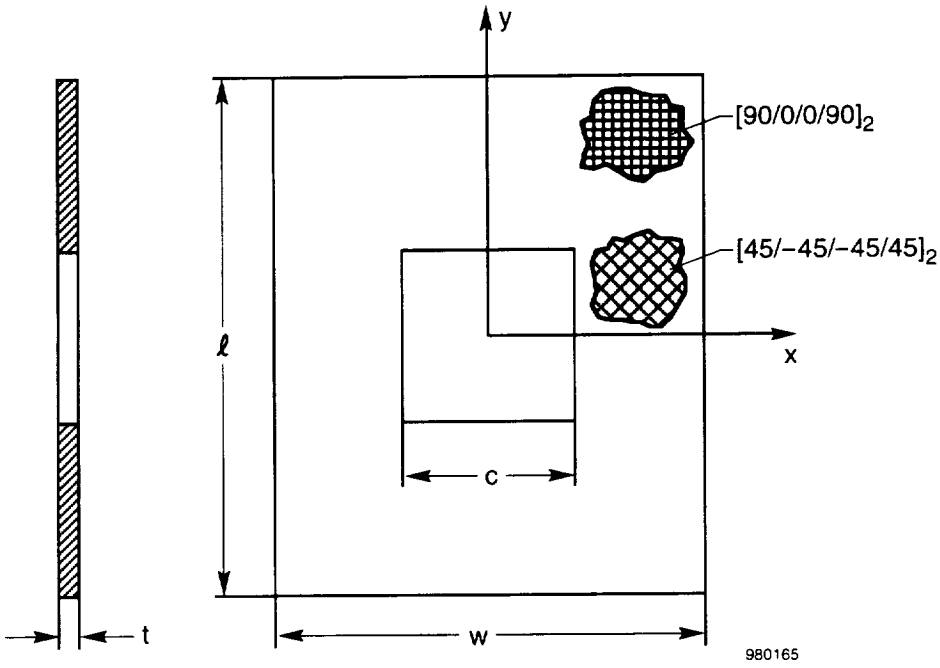

Figure 1. Metal-matrix composite plates with central cutouts.

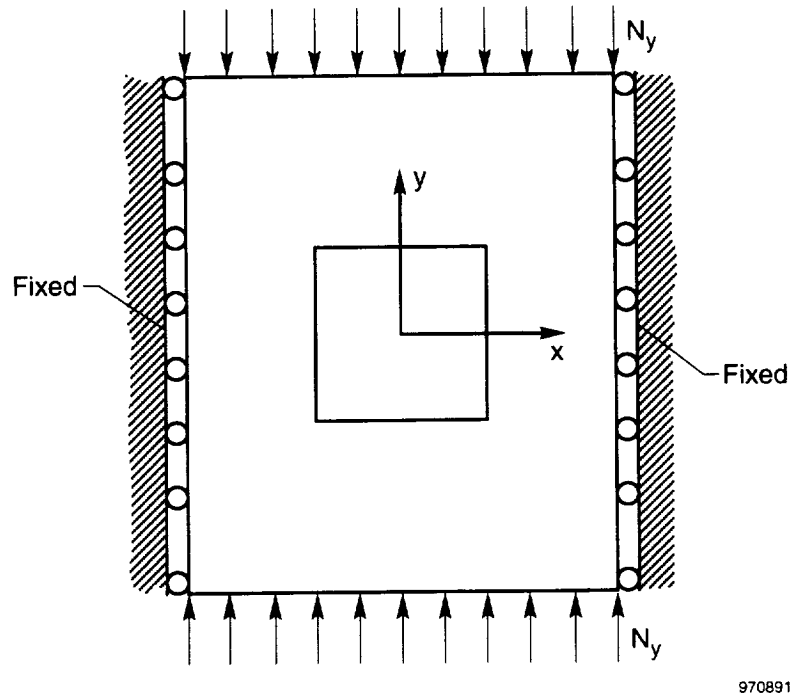

(a) Fixed case: two vertical edges have no in-plane transverse motions.

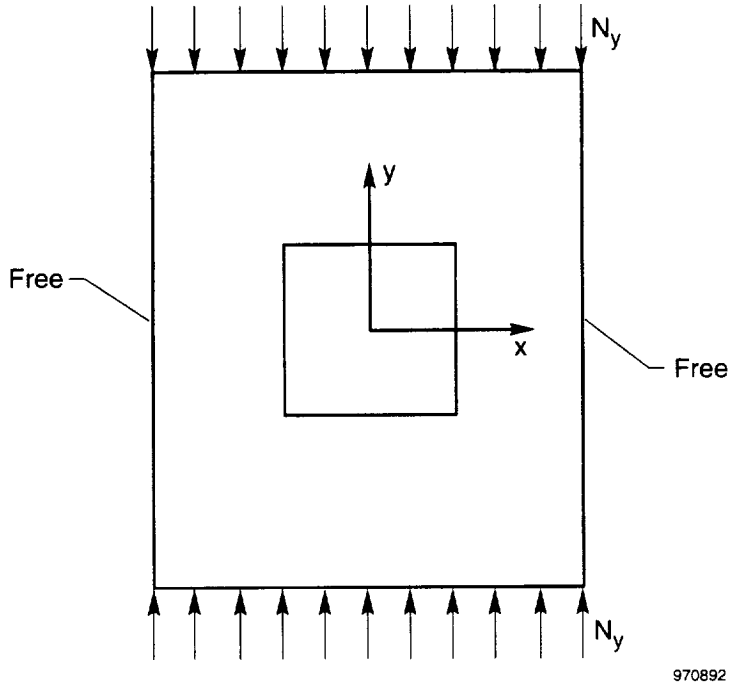

(b) Free case: two vertical edges have free in-plane transverse motions.

Figure 2. Fixed and free boundary conditions for two vertical edges; simply supported or clamped.

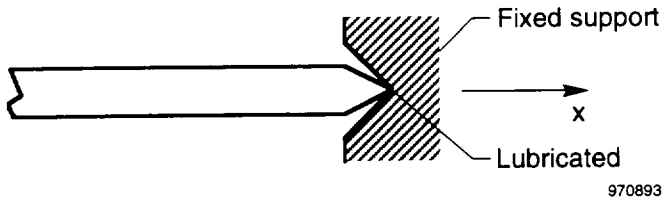

(a) 4S-fixed.

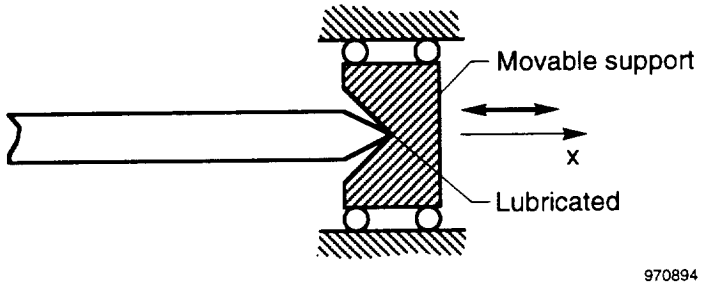

(b) 4S-free.

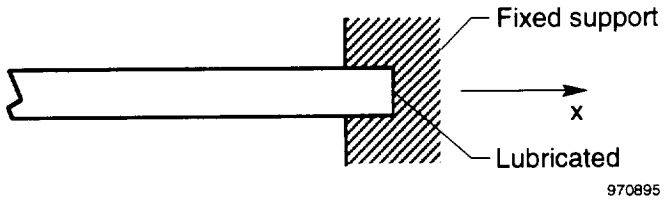

(c) 4C-fixed.

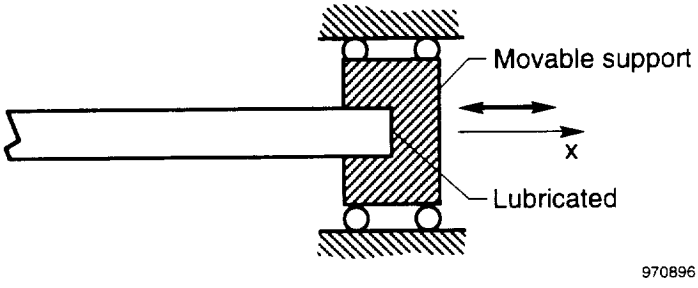

(d) 4C-free.

Figure 3. Four types of boundary conditions for the vertical edges.

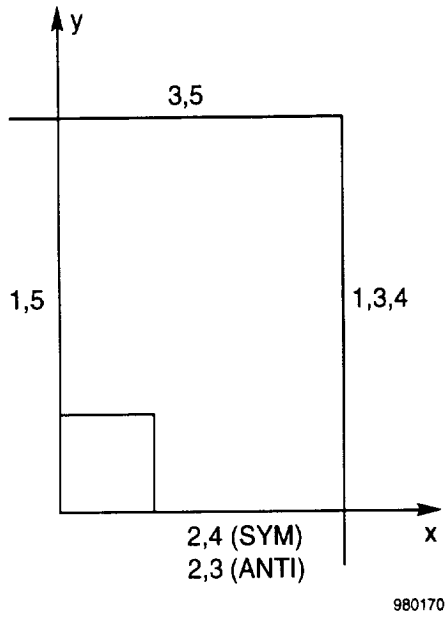

(a) 4S-fixed.

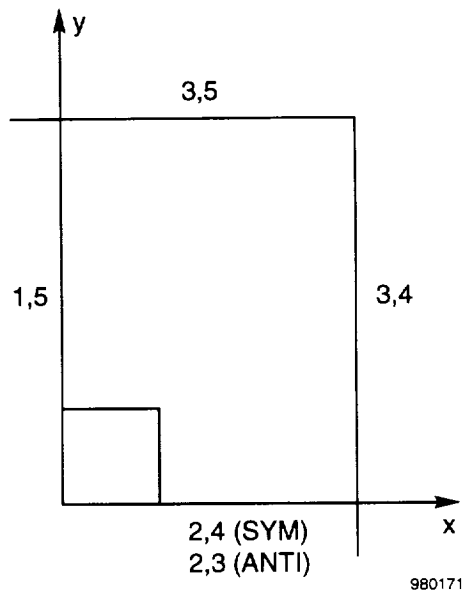

(b) 4S-free.

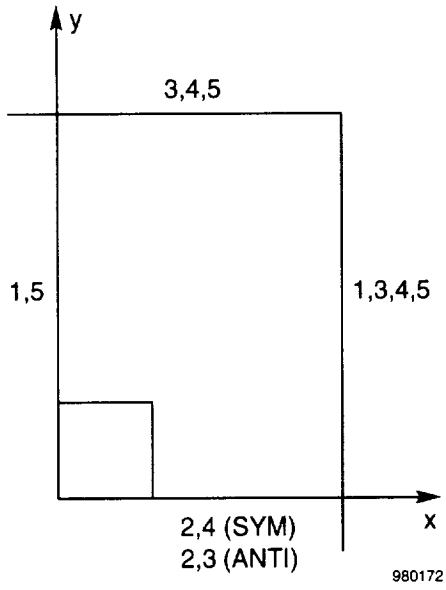

(c) 4C-fixed.

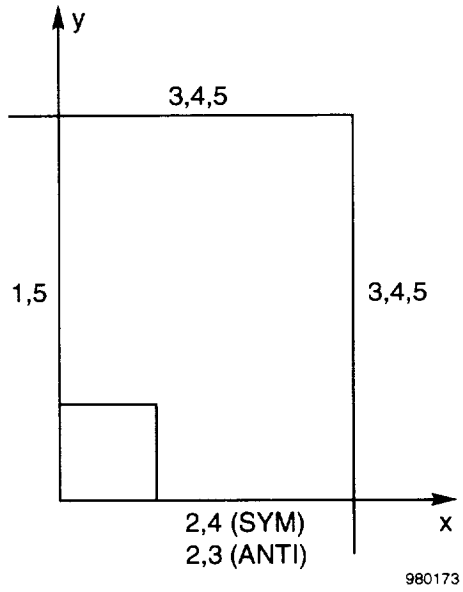

(d) 4C-free.

Figure 4. Constrained degrees of freedom for the four cases of plate boundary conditions; quarter panel; degree-of-freedom 6 is constrained for all cases.

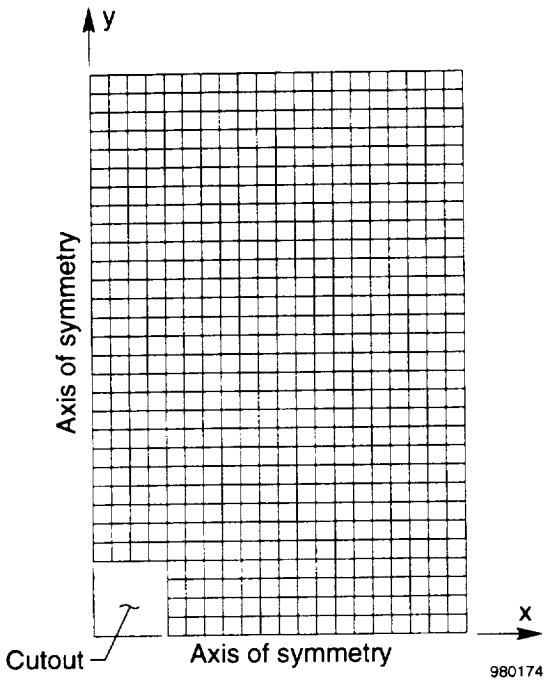

Figure 5. Quarter-panel finite-element model for rectangular MMC plate with square hole; $l/w = 1.5$; $c/w = 0.2$.

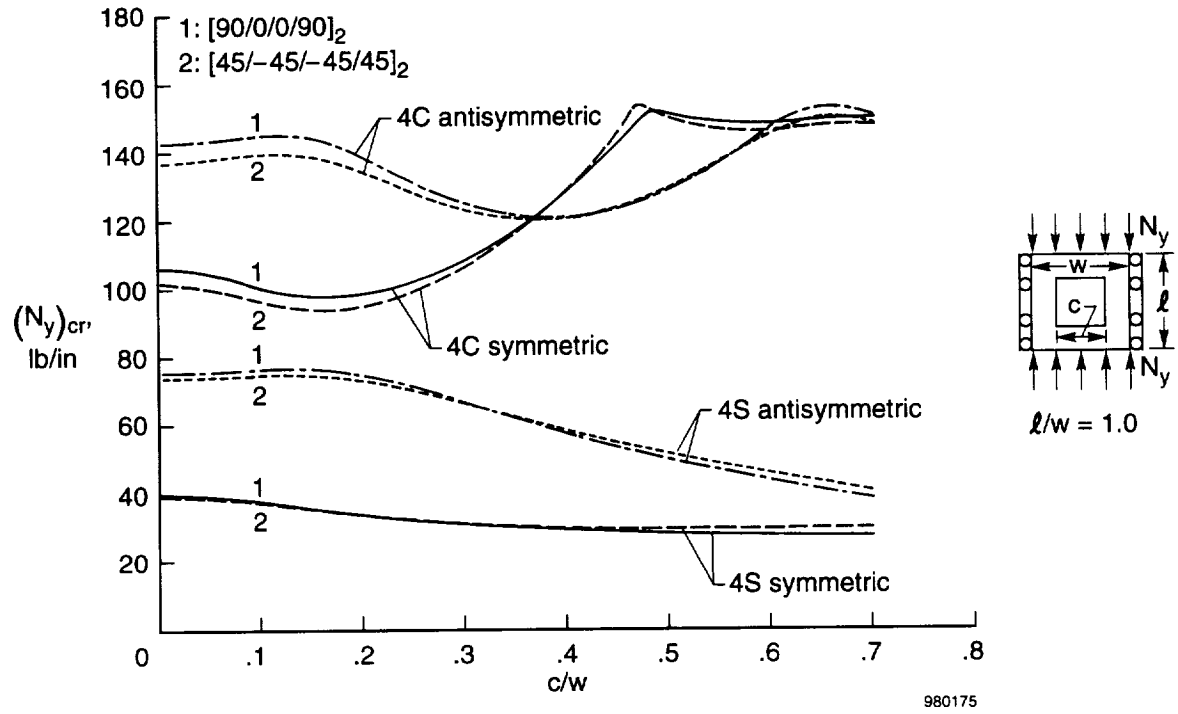

Figure 6. Compressive buckling loads as functions of hole size; l/w = 1.0; fixed edges.

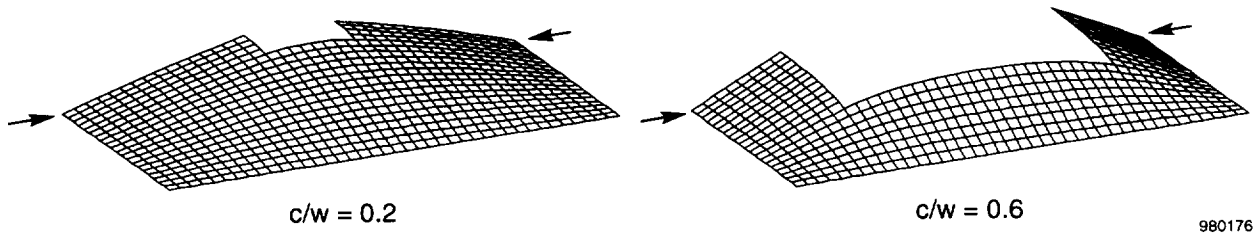

(a) 4S-fixed.

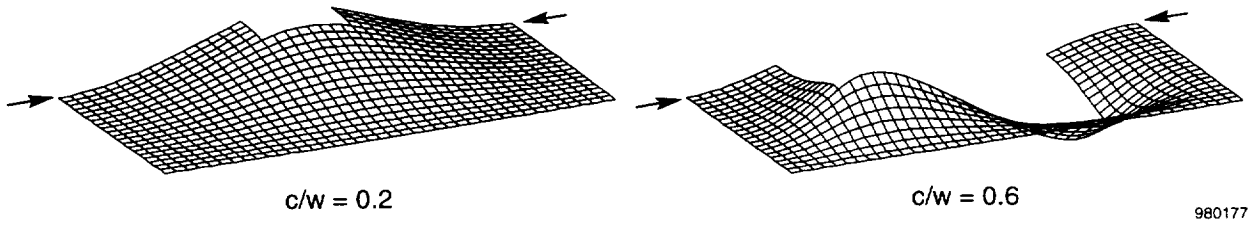

(b) 4C-fixed.

Figure 7. Buckled shapes of square plates with square holes under compression; l/w = 1.0; fixed edges.

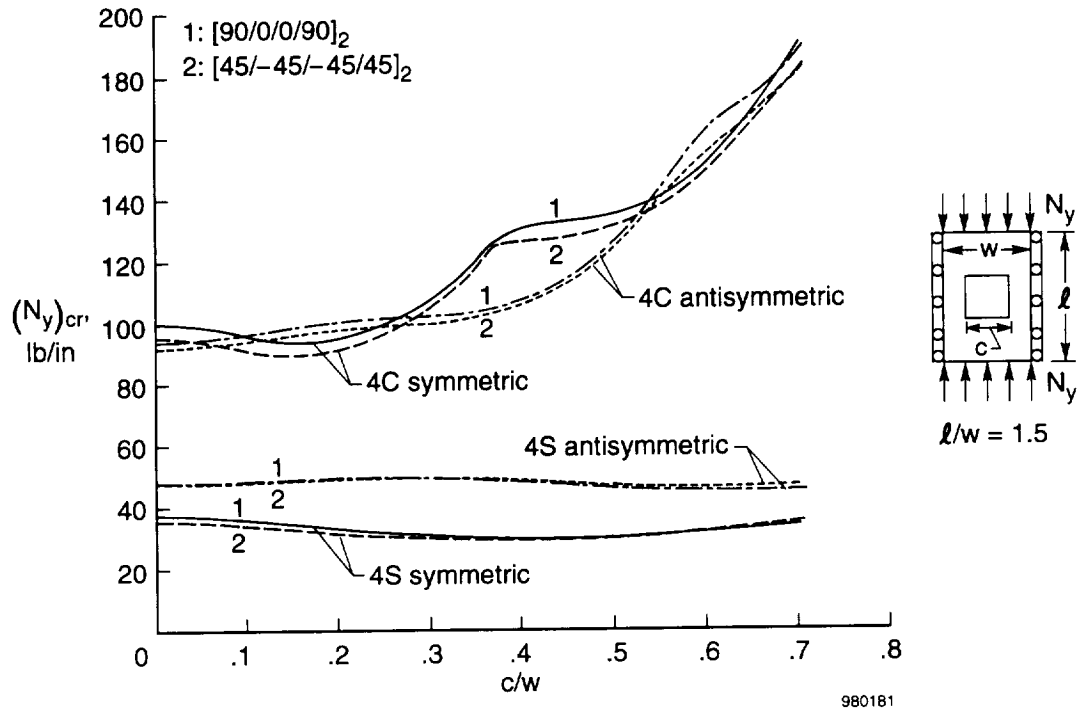

Figure 8. Compressive buckling loads as functions of hole size; l/w = 1.5; fixed edges.

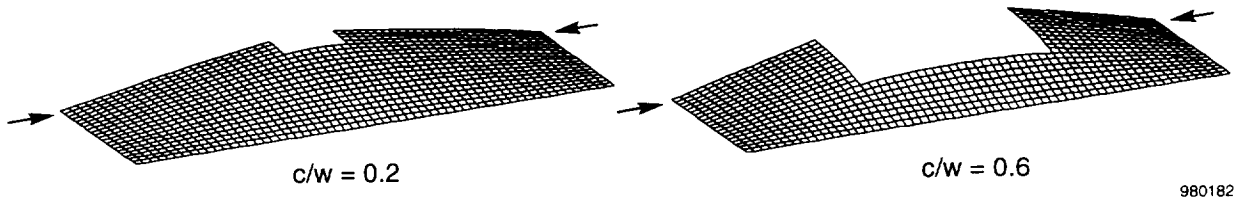

(a) 4S-fixed.

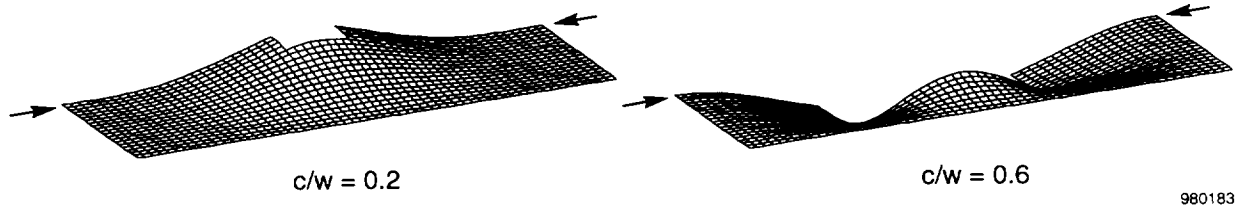

(b) 4C-fixed.

Figure 9. Buckled shapes of rectangular plates with square holes under compression; l/w = 1.5; fixed edges.

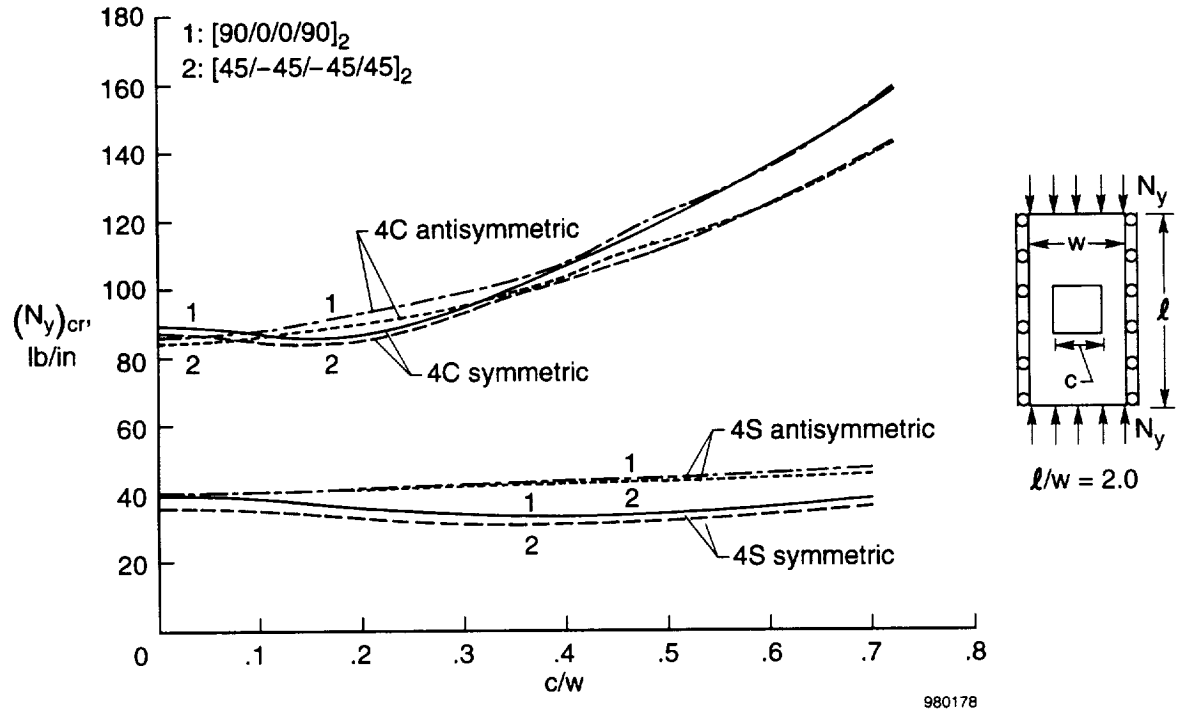

Figure 10. Compressive buckling loads as functions of hole size; l/w = 2.0; fixed edges.

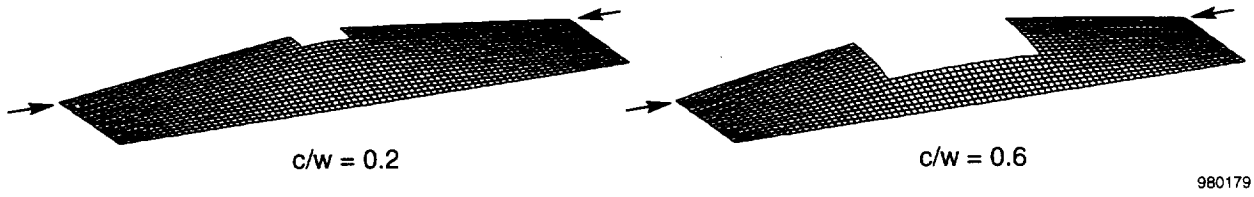

(a) 4S-fixed.

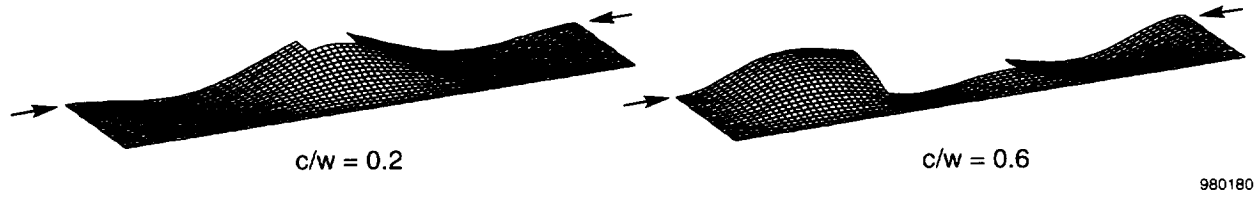

(b) 4C-fixed.

Figure 11. Buckled shapes of rectangular plates with square holes under compression; l/w = 2.0; fixed edges.

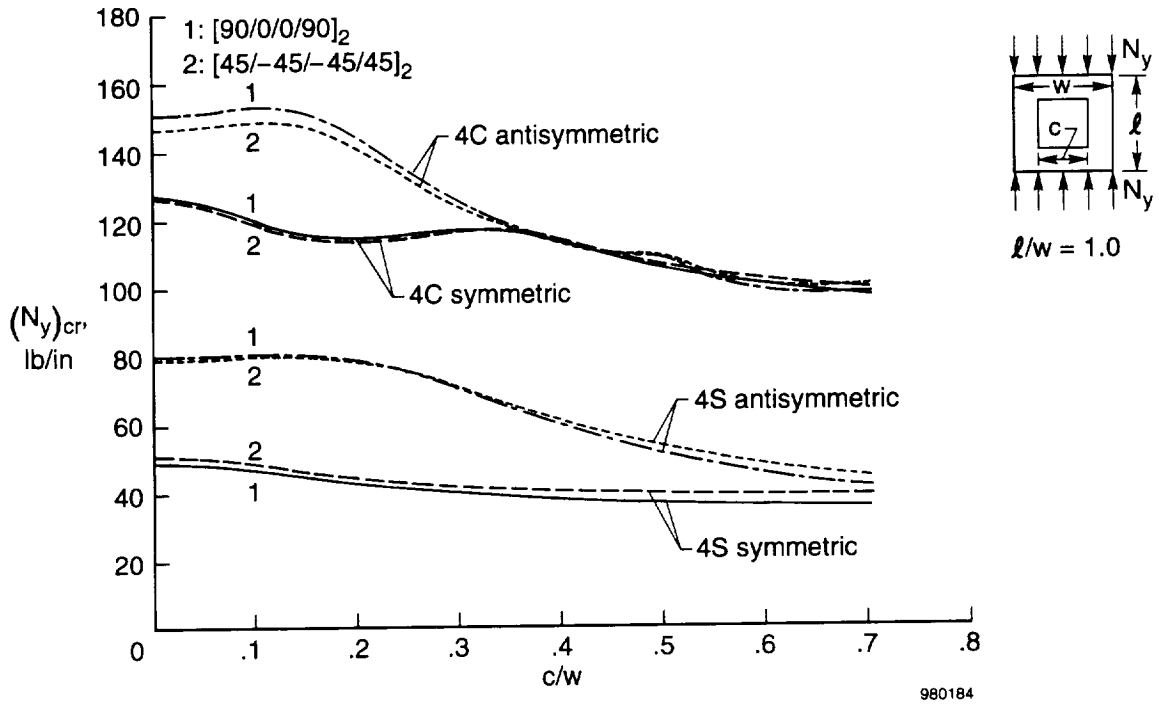

Figure 12. Compressive buckling loads as functions of hole size; l/w = 1.0; free edges.

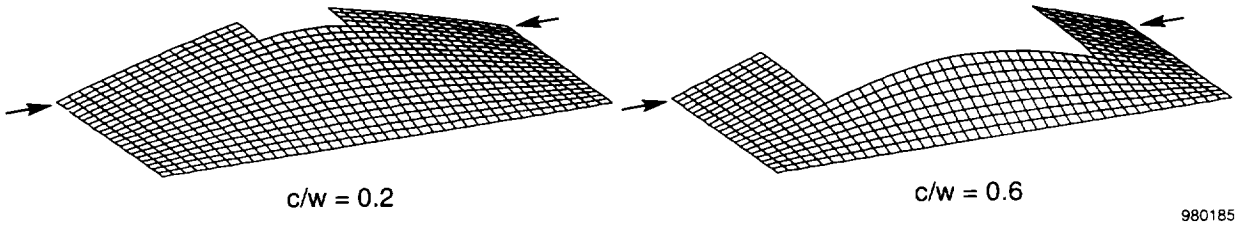

(a) 4S-free.

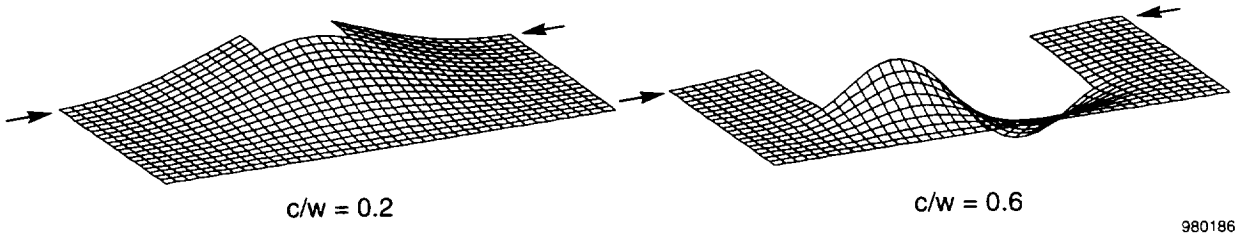

(b) 4C-free.

Figure 13. Buckled shapes of square plates with square holes under compression; l/w = 1.0; free edges.

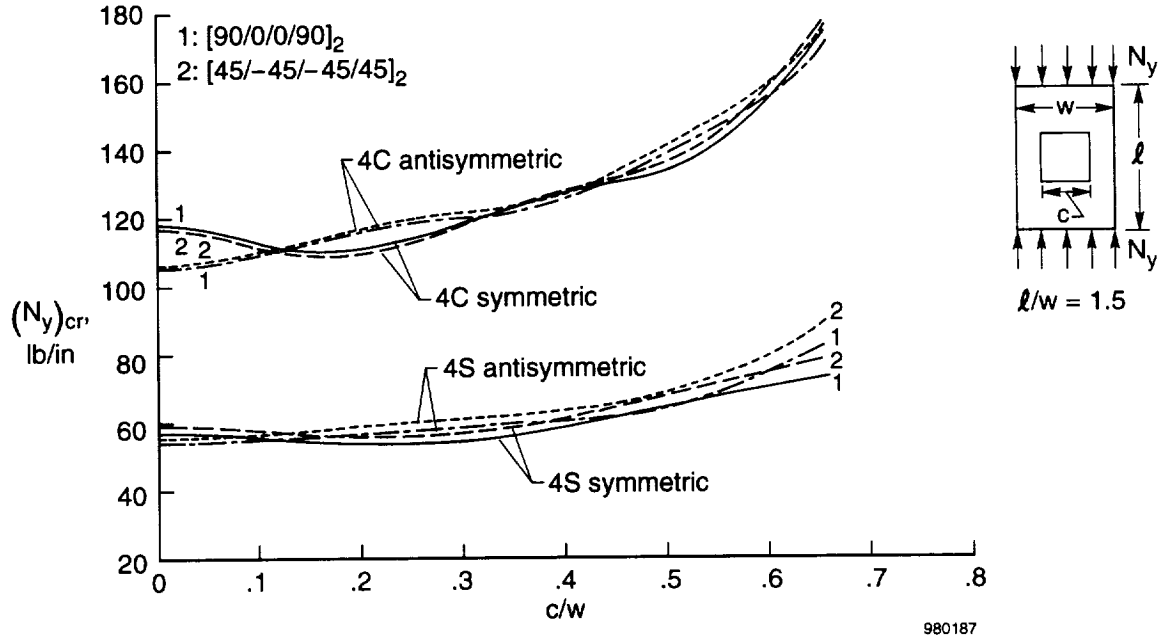

Figure 14. Compressive buckling loads as functions of hole size; l/w = 1.5; free edges.

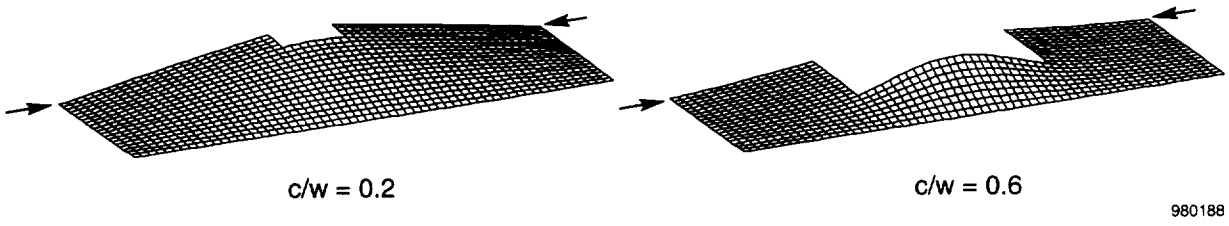

(a) 4S-free.

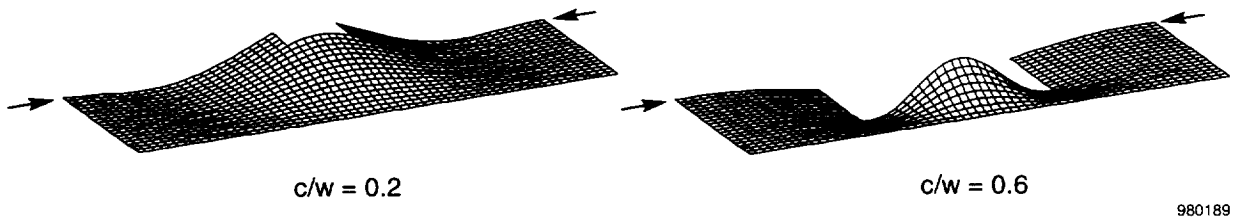

(b) 4C-free.

Figure 15. Buckled shapes of rectangular plates with square holes under compression; l/w = 1.5; free edges.

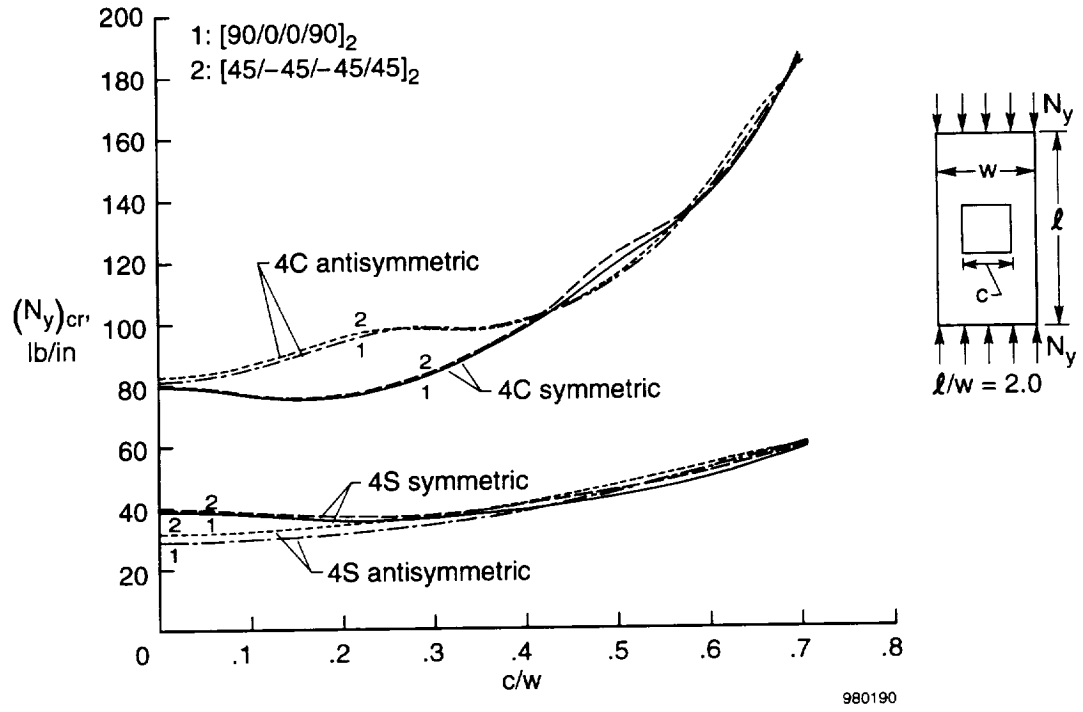

Figure 16. Compressive buckling loads as functions of hole size; l/w = 2.0; free edges.

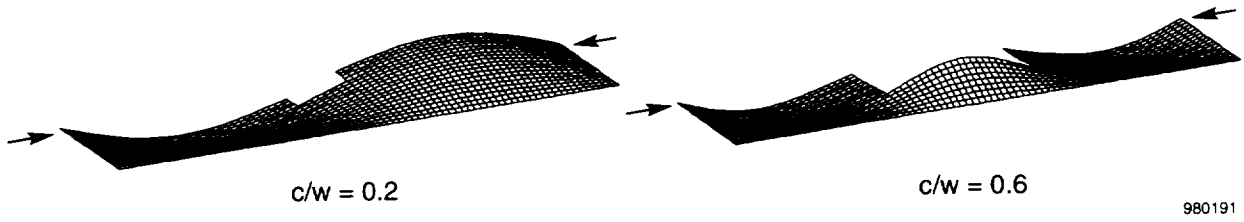

(a) 4S-free.

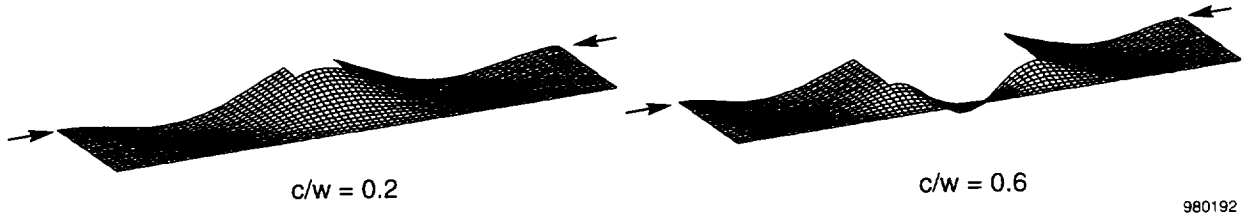

(b) 4C-free.

Figure 17. Buckled shapes of rectangular plates with square holes under compression; l/w = 2.0; free edges.

REPORT DOCUMENTATION PAGE

Form Approved
OMB No. 0704-0188

1. AGENCY USE ONLY (Leave blank)	2. REPORT DATE	3. REPORT TYPE AND DATES COVERED
	July 1998	Technical Paper

4. TITLE AND SUBTITLE

Anomalous Buckling Characteristics of Laminated Metal-Matrix Composite Plates with Central Square Holes

5. FUNDING NUMBERS

WU 522 32 34 00 RS 00 000 01

6. AUTHOR(S)

William L. Ko

7. PERFORMING ORGANIZATION NAME(S) AND ADDRESS(ES)

NASA Dryden Flight Research Center
P.O. Box 273
Edwards, California 93523-0273

8. PERFORMING ORGANIZATION REPORT NUMBER

H-2241

9. SPONSORING/MONITORING AGENCY NAME(S) AND ADDRESS(ES)

National Aeronautics and Space Administration
Washington, DC 20546-0001

10. SPONSORING/MONITORING AGENCY REPORT NUMBER

NASA/TP-1998-206559

11. SUPPLEMENTARY NOTES

12a. DISTRIBUTION/AVAILABILITY STATEMENT

Unclassified—Unlimited
Subject Category 39

12b. DISTRIBUTION CODE

13. ABSTRACT (Maximum 200 words)

Compressive buckling analysis was performed on metal-matrix composite (MMC) plates with central square holes. The MMC plates have varying aspect ratios and hole sizes and are supported under different boundary conditions. The finite-element structural analysis method was used to study the effects of plate boundary conditions, plate aspect ratio, hole size, and the composite stacking sequence on the compressive buckling strengths of the perforated MMC plates. Studies show that by increasing the hole sizes, compressive buckling strengths of the perforated MMC plates could be considerably increased under certain boundary conditions and aspect ratios ("anomalous" buckling behavior); and that the plate buckling mode could be symmetrical or antisymmetrical, depending on the plate boundary conditions, aspect ratio, and the hole size. For same-sized plates with same-sized holes, the compressive buckling strengths of the perforated MMC plates with $[90/0/0/90]_2$ lamination could be as much as 10 percent higher or lower than those of the $[45/-45/-45/45]_2$ laminations, depending on the plate boundary conditions, plate aspect ratios, and the hole size. Clamping the plate edges induces far stronger "anomalous" buckling behavior (enhancing compressive buckling strengths at increasing hole sizes) of the perforated MMC plates than simply supporting the plate edges.

14. SUBJECT TERMS	15. NUMBER OF PAGES
Anomalous buckling, Aspect ratio effect, Edge support effect, Hole size effect, Metal-matrix composites, Square cutout	27
	16. PRICE CODE: A03

17. SECURITY CLASSIFICATION OF REPORT	18. SECURITY CLASSIFICATION OF THIS PAGE	19. SECURITY CLASSIFICATION OF ABSTRACT	20. LIMITATION OF ABSTRACT
Unclassified	Unclassified	Unclassified	Unlimited